Facile route to synthesise larger mesoporous nickel silicate coated on carbon nanotubes and application for dye removal

Peixiong Xia, Min Zhang, Jing Zheng, Yue Zheng, Jingli Xu

College of Chemistry and Chemical Engineering, Shanghai University of Engineering Science, Shanghai 201620, People's Republic of China
E-mail: zhangmin@sues.edu.cn

Published in Micro & Nano Letters; Received on 1st November 2013; Revised on 18th February 2014; Accepted on 27th February 2014

Presented is a facile route to synthesise mesoporous nickel silicate coated on carbon nanotubes (CNTs) with a larger hole based on the mesoporous silica coated on the CNTs, the pore size of the mesoporous silica coated on the CNTs was enlarged from 2.72 to 7.8 nm after a hydrothermal reaction with nickel ions. Compared with other work for expanding the size of the pore, the authors' presented method is low cost, simple and highly efficient. More importantly, this method shows great potential in applying other types of mesoporous materials such as SBA-15 and so on, all of which indicate that both the mesoporous nickel silicate coated on the CNTs and the mesoporous silica coated on the CNTs could serve as good candidates for adsorption on the organic pollutants.

1. Introduction: Organic dyes are widely used in the textile, paper, plastic and leather industries to colour commercial products. However, organic dyes in industrial wastewater may cause serious environmental problems because of their toxicity and poor biodegradability, which may risk humankind's health [1–5]. Moreover, the dyes may significantly affect photosynthetic activity in aquatic life because of a reduced light penetration and may also be toxic to aquatic life because of the presence of aromatic, metal and chloride groups in their structures. These synthetic dyes show great differences in chemical composition, molecular weight and toxicity, and they are mostly stable and resistant to biodegradation because of their complex aromatic molecular structures. Even more important, these dyes are very difficult to remove from wastewater by chemical or biological degradation methods, because of their stability against heat, light and many chemical reagents.

Accordingly, it is necessary to find an efficient way to separate and remediate these organic pollutants. Among all the technologies applied in the removal of the organic pollutants, the role of fly ash, the photocatalytic oxidation of the organic pollutants [6, 7] and adsorption are shown to be the procedures of choice for the removal of the dyes. In addition, adsorption has been observed to be an effective process for colour removal from dye wastewater [8, 9]. Several studies have been performed to investigate the use of low-cost adsorbents such as rice husk, poplar leaf, clay, carbon and silica for dye removal [10–12]. However, these adsorbents have generally low adsorption capacities and are difficult to separate from the treated water because of their small particle sizes. Therefore, it is desirable to explore the facile adsorbent materials for the removal of organic dye pollutants with a high efficiency and at a low cost.

Recently, silicate materials have been widely used in catalysis and adsorption owing to their low cost, stability, environmentally benign nature and excellent properties [13–17]. For adsorption, the mesoporous materials may be advantageous in terms of the adsorption kinetics. The properties of the mesoporous materials such as pore size, pore geometry and surface chemistry can be tailored, which allows us to precisely design the support for the desired application. In addition, a high specific surface area and the porous structures are two critical factors that enhance the interaction between the pollutants and the adsorption sites for high adsorption capacities. Therefore, more work has been focused on the mesoporous materials for adsorption. In particular, the magnesium silicate nanomaterials can be used as they are highly efficient adsorbents for adsorbing the organic pollutants, the radioactive isotopes and the heavy-metal cations [18]. It is worth noting that the metal silicates can resist the basic etching in a high alkali solution whereas the silica materials do not [19], which will make widespread the use of metal silicates for the adsorption of organic pollutants in a harsh environment.

Meanwhile, compared with the other dimensional materials such as the zero-dimensional materials (0D), 1D silicate nanotubes with mesoporous shells have better mechanical strength and a shorter diffusion path for mass transport, and are thereby more suitable for adsorption as well as easier centrifugation. Zhu *et al.* [20, 21] have developed a facile and efficient template engaged conversion route to grow the arrays of the CuS nanoneedles and the Ni_3S_2 nanosheets on the carbon nanotubes' (CNTs) backbone with the hierarchical nanostructures which exhibit interesting properties for energy storage and hydrogen production. More recently, Song *et al.* have synthesised magnetic magnesium silicate nanotubes and metal silicate nanotubes and they showed very good adsorption properties for the heavy metal ions [22, 23]. Our group have also reported that the SiO_2 shells coated on the CNTs exhibited a highly porous structure by using the cationic surfactant CTAB, and have explored the application of a size-selective adsorption of the biomacromolecules [24]. Inspired by the above work, we have developed a facile way to synthesise the mesoporous nickel silicate coated on the CNTs with a larger hole, and the pore size of the mesoporous silica coated on the CNTs was enlarged from 2.72 to 7.8 nm, and methylene blue (MB) was also selected to evaluate the adsorption ability between the two kinds of materials. Compared with the other work, our method is low cost, simple and has a high efficiency, and more importantly, this method shows great potential in applying other types of the mesoporous materials such as SBA-15 and so on. The typical synthetic process is summarised in Fig. 1.

2. Experimental

2.1. Materials: Multiwalled CNTs (MWCNTs) with a mean diameter of 60–80 nm were provided by the Shenzhen Nanotech Port Co. Ltd. Tetraethoxysilane (TEOS, 95%) was obtained from the Alfa Aesar Chemical Company, which was used directly without further purification. The other chemical reagents were purchased from the Shanghai Chemical Reagent Company.

doi: 10.1049/mnl.2013.0634

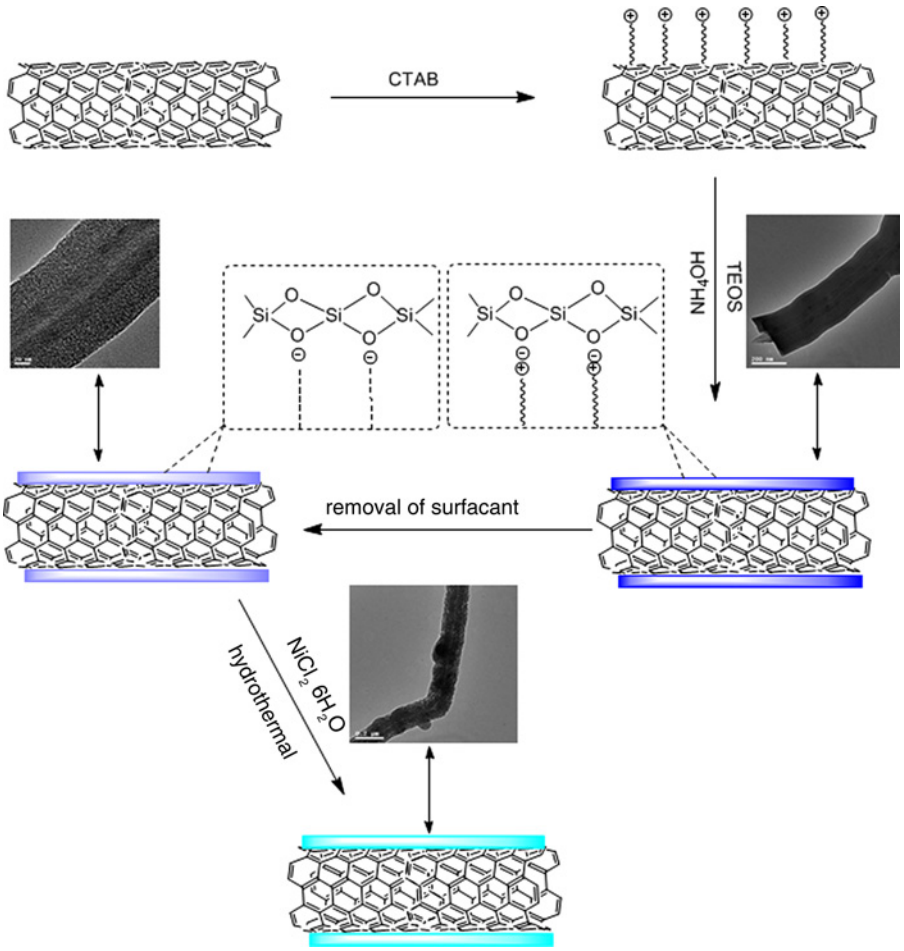

Figure 1 *Synthetic procedure of the mesoporous nickel silicate coated CNTs by the hydrothermal method based on the mesoporous silica (MCM-41) coated CNTs*

2.2. Synthesis of the mesoporous SiO_2 on the CNTs: The mesoporous silica coating of the CNTs was synthesised according to our previous paper [24]. Specifically, 100 mg CNTs and 1000 mg CTAB were dispersed into 30 ml of deionised water, and the mixture was sonicated for 1 h. Next, the above mixture was added to 80 ml of anhydrous ethanol and further sonicated for 0.5 h to form a stable dispersion. Immediately, 2 ml of $NH_3{\cdot}H_2O$ was added into the as-prepared CNTs dispersion. Then, a TEOS solution (1 ml of TEOS in 40 ml of ethanol) was dropped into the CNTs dispersion under mechanical stirring, and the reaction mixture was stirred for another 12 h without sonication. Finally, the CNTs solution was centrifuged and washed with ethanol. The process results in the formation of a uniform and thick layer of silica on every individual CNT. The surfactants were removed by a fast and efficient ion exchange method (1.2 g of NH_4NO_3 in 60 ml of ethanol) to obtain SiO_2 coated CNTs with a mesoporous structure.

2.3. Synthesis of the mesoporous nickel silicate coated CNTs: The synthesis procedure of the mesoporous nickel silicate coated CNTs was achieved by the hydrothermal method. Taking the as-prepared product 100 mg SiO_2 coated CNTs with a mesoporous structure and 100 mg of $NiCl_2{\cdot}6H_2O$, added into a vessel with 35 ml of H_2O, hydrothermaled at 180°C for 7.5 h, the nickel silicate coated on the CNTs was obtained. The resultant products were separated and collected, followed by washing with deionised water and ethanol three times, respectively. Then, the obtained powders were dried at 60°C overnight.

2.4. Dye adsorption experiments: To investigate the rebinding capacity, 10 mg of the as-prepared products was incubated with 3 ml of MB solution at 100 $mg{\cdot}l^{-1}$ for 1 h. After centrifugation, the concentration of MB in the supernatant was determined by using a UV/vis spectrophotometer. The amount of the dyes adsorbed onto the as-prepared products was calculated from the differences in the dye concentrations before and after incubation on the rotator (150 rpm) with the silica-coated CNTs.

2.5. Characterisation: A Tecnai G^2 20 S-TWIN microscope was used to obtain the transmission electron microscope (TEM) images of SiO_2 at the CNTs composites. The morphology of the samples was obtained by a scanning electron microscope (FEI Quanta, Sweden). N_2 adsorption–desorption analysis was performed at 77 K on a Micromeritics TriStar 3000 apparatus. The surface area was determined by using the Brunauer-Emmett-Teller equation, and the pore diameter was estimated by using the Barrett-Joyner-Halenda model. A thermogravimetric analysis (TGA) was performed for the powder samples (~1.2 mg) with a heating rate of 10°C·min^{-1} by using a Netzsch STA 409 (Germany) thermogravimetric analyser under an atmosphere of up to 800°C.

3. Results and discussion

Synthesis and characterisation of the mesoporous nickel silicate coated on the CNTs: As illustrated in Fig. 1, the CNTs at the CTAB at SiO_2 were firstly synthesised through a sol–gel method. After extraction by a fast and efficient ion exchange method, the mesoporous silica coated on the CNTs was obtained. Finally, the

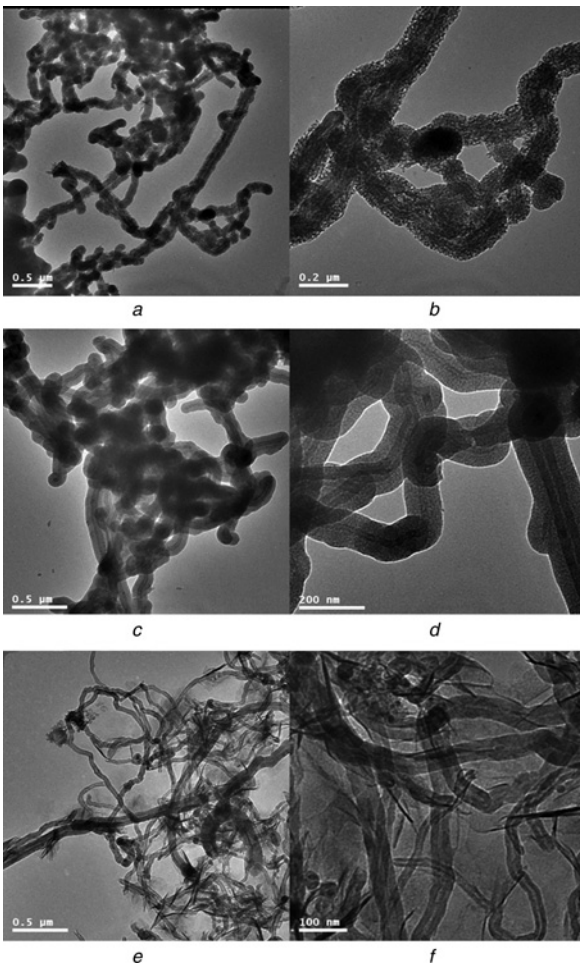

Figure 2 *TEM images*
a, b Mesoporous nickel silicate coated on the CNTs
c, d Mesoporous silica coated on the CNTs
e, f Products hydrothermaled for 7.5 h

mesoporous SiO_2 shell of the CNTs was transformed into nickel silicate with a larger pore under the hydrothermal conditions. The morphological structure of the mesoporous CNTs at SiO_2 before and after the hydrothermal reaction with $NiCl_2$ were characterised by TEM, respectively. The TEM image shows the change in the CNTs before (Figs. 2*c* and *d*) and after the hydrothermal reaction (Figs. 2*a* and *b*). Before the hydrothermal reaction, a 45 nm-thick SiO_2 layer covered the CNTs and the surface of silica was smooth. After the hydrothermal reaction, a mesoporous nickel silicate layer was obtained and the thickness of the coating was kept as before. However, the surface of nickel silicate was rough and loose.

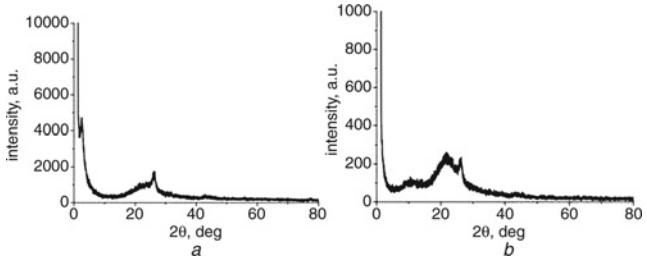

Figure 3 *XRD patterns*
a Mesoporous silica coated CNTs
b Mesoporous nickel siliceous coated on the CNTs

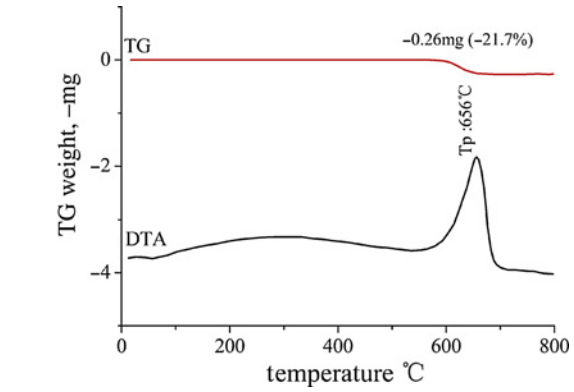

Figure 4 *TG/DSC data of the mesoporous nickel siliceous coated on the CNTs*

The XRD patterns for the mesoporous silica coated CNTs showed a reflection in the small-angle region (Fig. 3*a*). The (100) diffraction peaks of the mesoporous silica coated on the CNTs were $2\theta = 2.6°–3.4°$, which indicated the presence of a mesoporous structure, whereas the peaks for mesoporous nickel siliceous coated on the CNTs at $2\theta = 2.6°–3.4°$ were not observed. This indicates that the order of the mesoporous structures was destroyed by the hydrothermal reaction. As shown in Fig. 3*b*, the representative XRD pattern of the mesoporous nickel silicate nanostructure indicates that both the CNTs and nickel silicate existed. However, because of the low concentration of nickel silicate, only one intensity peak located at 20° can be clearly observed. The nickel silicate is indexed to be nickel silicate hydroxide hydrate hexagonal phase (JCPDS No. 43–0664) and such a substance is defined as nickel silicate in this Letter. Based on the combined XRD and TEM, the rough and the loose nickel silicate shells have been successfully fabricated by using such a simple method.

The TGA of the nickel silicate coated on the CNTs showed one weight loss, which occurred at about 656°C, corresponds to the oxidation of the CNTs embedded in the CNTs at SiO_2 and a 21.7% weight loss was observed. It is proved that the thermal stability of the CNTs after being coated by nickel silicate has been much improved. Thus, from the TGA results, we can conclude that a nickel silicate coated CNTs composite was indeed obtained via this method (Fig. 4). The changes in the pore properties of the mesoporous silica coated on the CNTs were also verified by the results of the nitrogen adsorption–desorption measurements. Fig. 5 shows the nitrogen adsorption–desorption isotherms and the corresponding pore size distributions for the mesoporous silica coated on the CNTs (MSCNTs) and the mesoporous nickel silicate coated on the CNTs (MNSCNTs). The isotherms are type *IV* curves and the specific surface area, the average pore size and the pore volumes of all the samples are summarised: for the MSCNTs, these ranged from 831 $m^2\ g^{-1}$, 27.2 A° and 0.56 $cm^3\ g^{-1}$,

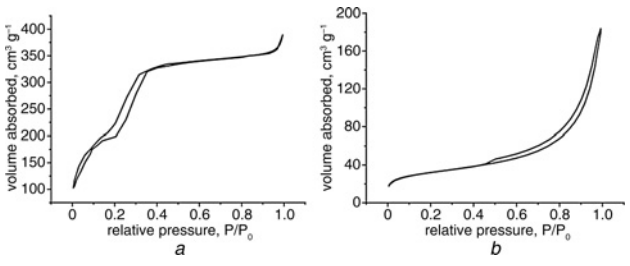

Figure 5 *N_2 adsorption–desorption isotherms*
a For mesoporous CNTs at SiO_2 and
b For mesoporous CNTs at SiO_2–$NiCl_2$

doi: 10.1049/mnl.2013.0634

respectively; for the pore-expanded MNSCNTs, they ranged from 113 m^2 g^{-1}, 78.5 A° and 0.26 cm^3 g^{-1}. The pore sizes increased substantially, being 2.8 times larger than the original values, respectively. To explore the reason for a larger hole generated on the mesoporous silica coated on the CNTs, a possible mechanism was also proposed. At first, the nickel ion was absorbed into the pore of the mesoporous silica coated on the CNTs, driven by an interfacial reaction between the nickel ion and the silica shell. The nickel silicate nanomaterials were generated around every pore of the mesoporous silica, the previous adjacent mesoporous silica pores were merged into a nickel silicate pore of a larger size. In contrast to the previous paper, no alkaline solution was introduced to the reaction system, and the hierarchical nanostructures were not observed in this Letter. This phenomenon fully indicates that the morphology of the nickel silicate coated on the CNTs could be controlled by controlling the pH of the system. To further explore the formation mechanism of the MNSCNTs, the reaction time was also extended to 20 h. Unfortunately, the mesoporous silica coated on the CNTs was totally transformed into siliceous nickel, and denuded from the surface of the CNTs, which is shown in Fig. 2*e*. Hence, the time of the reaction is the key to the formation of the MNSCNTs. In our Letter, the time was set as 7.5 h.

The as-prepared mesoporous CNTs at SiO_2 and the nickel silicate coated on the CNTs were used as the absorbents in the dyes' treatment. The organic dyes have been considered as a primary toxic pollutant in the water resources. In this Letter, to illustrate the high uptake capacity of the two kinds of mesoporous materials, the CNTs at the CTAB at SiO_2 were studied as the control. MB, a typical organic dye, was also chosen as a testing organic pollutant. The absorption spectra of a solution of MB in the presence of different kinds of CNTs at SiO_2 were also monitored by a UV–vis spectrophotometer (Fig. 6). The obvious colour change of the aqueous dye was observed (Fig. 6, inset). We believe that the efficient removal is mainly attributed to its small pore size and the high surface area of two kinds of mesoporous CNTs at SiO_2. It is observed that the amount of adsorption on MB for the mesoporous nickel silicate (Fig. 6*c*) is lower than that of the mesoporous silica coated on the CNTs (Fig. 6*d*), which may be because of the differences of the surface area. In contrast to the two kinds of mesoporous CNTs at SiO_2, the CNTs at the CTAB at SiO_2 showed a smaller adsorption capacity (Fig. 6*b*). This result demonstrated that the two kinds of mesoporous materials have a much greater MB removal efficiency than that of the CNTs at the CTAB at SiO_2. Furthermore, it is worth noting that the mesoporous CNTs at the SiO_2 could be activated again by simple calcinations at 350°C in air for 2 h [25–27]. After regenerating three times, the removal efficiency of the dyes was still kept above 90%.

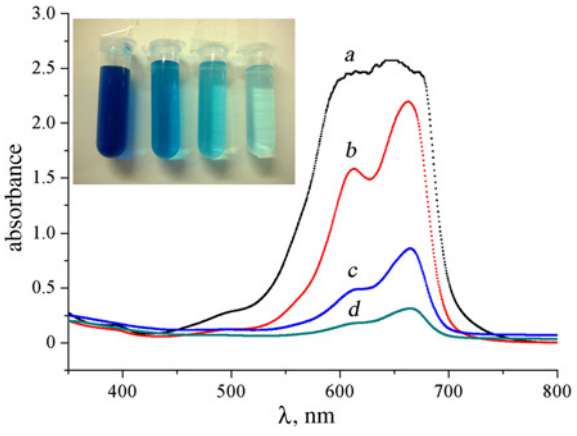

Figure 6 *Absorption spectra Solution of MB (a), in the presence of the CNTs at the CTAB at SiO_2 (b), mesoporous CNTs at SiO_2–$NiCl_2$ (c), mesoporous CNTs at SiO_2 (d)*

4. Conclusions: In summary, a facile method has been developed to synthesise the mesoporous nickel silicate coated on the CNTs with a larger pore. It was found that the two kinds of mesoporous silica coated on the CNTs exhibit an excellent performance for the removal of MB by adsorption. The spent sample can be readily regenerated and reused after simple calcinations at high temperatures and, more importantly, this method shows great potential in applying the other types of mesoporous materials such as SBA-15 and so on, which will broaden the range of the method for expanding the hole size of the mesoporous materials.

5. Acknowledgments: The authors appreciate financial support by the National Natural Science Foundation of China (21305086), the Natural Science Foundation of Shanghai City (13ZR141830), the Research Innovation Program of the Shanghai Municipal Education Commission (14YZ138), the Special Scientific Foundation for Outstanding Young Teachers in Shanghai Higher Education Institutions (2014Z10856016) and the Start-up Funding of Shanghai University of Engineering Science.

6 References

[1] Zhang P., An Q., Guo J., Wang C.-C.: 'Synthesis of mesoporous magnetic Co-Nps/carbon nanocomposites and their adsorption property for methyl orange from aqueous solution', *J. Colloid Interface Sci.*, 2013, **389**, (1), pp. 10–15

[2] Niu P., Hao J.: 'Fabrication of titanium dioxide and tungstophosphate nanocomposite films and their photocatalytic degradation for methyl orange', *Langmuir*, 2011, **27**, (22), pp. 13590–13597

[3] Sharma Y.C., Upadhyay S.N: 'Removal of a cationic dye from wastewaters by adsorption on activated carbon developed from coconut coir', *Energy Fuels*, 2009, **23**, (6), pp. 2983–2988

[4] Pal S., Ghorai S., Das C., Samrat S., Ghosh A., Panda A.B.: 'Carboxymethyl tamarind-G-poly(acrylamide)/silica: a high performance hybrid nanocomposite for adsorption of methylene blue dye', *Ind. Eng. Chem. Res.*, 2012, **51**, (48), pp. 15546–15556

[5] Richardson S.D.: 'Environmental mass spectrometry: emerging contaminants and current issues', *Anal. Chem.*, 2008, **80**, (12), pp. 4373–4402

[6] Ahmaruzzaman M.: 'Role of fly ash in the removal of organic pollutants from wastewater', *Energy Fuels*, 2009, **23**, (3), pp. 1494–1511

[7] Chen X., Ma W., Li J., *ET AL.*: 'Photocatalytic oxidation of organic pollutants catalyzed by an iron complex at biocompatible pH values: using O_2 as main oxidant in a Fenton-like reaction', *J. Phys. Chem. C*, 2011, **115**, (10), pp. 4089–4095

[8] Rastogi K., Sahu J.N., Meikap B.C., Biswas M.N.: 'Removal of methylene blue from wastewater using fly ash as an adsorbent by hydrocyclone', *J. Hazardous Mater.*, 2008, **158**, (2–3), pp. 531–540

[9] Ramakrishna K.R., Viraraghavan T.: 'Dye removal using low cost adsorbents', *Water Sci. Technol.*, 1997, **36**, (2–3), pp. 189–196

[10] Noroozi B., Sorial G.A., Bahrami H., Arami M.: 'Equilibrium and kinetic adsorption study of a cationic dye by a natural adsorbent – silkworm pupa', *J. Hazardous Mater.*, 2007, **139**, (1), pp. 167–174

[11] Nam K.H., Tavlarides L.L.: 'Synthesis of a high-density phosphonic acid functional mesoporous adsorbent: application to chromium (III) removal', *Chem. Mater.*, 2005, **17**, (6), pp. 1597–1604

[12] Upadhyayula V.K.K., Deng S., Mitchell M.C., Smith G.B.: 'Application of carbon nanotube technology for removal of contaminants in drinking water: a review', *Sci. Total Environ.*, 2009, **408**, (1), pp. 1–13

[13] Mizutani M., Yamada Y., Nakamura T., Yano K.: 'Anomalous pore expansion of highly monodispersed mesoporous silica spheres and its application to the synthesis of porous ferromagnetic composite', *Chem. Mater.*, 2008, **20**, (14), pp. 4777–4782

[14] Rasoul M., Rajabi M.H., Ara M.H.M.: 'Structural and optical characteristics of silica nanotubes using CNTs as template', *Nano Micro Lett.*, 2010, **2**, (4), pp. 268–271

[15] Slowing I.I., Vivero-Escoto J.L., Wu C.-W., Lin V.S.Y.: 'Mesoporous silica nanoparticles as controlled release drug delivery and gene transfection carriers', *Adv. Drug Deliv. Rev.*, 2008, **60**, (11), pp. 1278–1288

[16] Lu X., Liu H., Deng C., Yan X.: 'Facile synthesis and application of mesoporous silica coated magnetic carbon nanotubes', *Chem. Commun.*, 2011, **47**, (4), pp. 1210–1212

[17] Mizutani M., Yamada Y., Yano K.: 'Pore-expansion of monodisperse mesoporous silica spheres by a facile surfactant exchange method', *Chem. Commun.*, 2007, **5**, (5), pp. 1172–1174
[18] Fang Q.-R., Zhu G.-S., Xue M., *ET AL.*: 'Microporous metal–organic framework constructed from heptanuclear zinc carboxylate secondary building units', *Chem. – A Eur. J.*, 2006, **12**, (14), pp. 3754–3758
[19] Fang Q., Xuan S., Jiang W., Gong X.: 'Yolk-like micro/nanoparticles with superparamagnetic iron oxide cores and hierarchical nickel silicate shells', *Adv. Funct. Mater.*, 2011, **21**, (10), pp. 1902–1909
[20] Zhu T., Xia B., Zhou L., Lou X.W.: 'Arrays of ultrafine CuS nanoneedles supported on a CNT backbone for application in supercapacitors', *J. Mater. Chem.*, 2012, **22**, (16), pp. 7851–7855
[21] Zhu T., Wu H.B., Wang Y., Xu R., Lou X.W.: 'Formation of 1d hierarchical structures composed of Ni_3S_2 nanosheets on CNTs backbone for supercapacitors and photocatalytic H2 production', *Adv. Energy Mater.*, 2012, **2**, (12), pp. 1497–1502
[22] Cao C.-Y., Wei F., Qu J., Song W.-G.: 'Programmed synthesis of magnetic magnesium silicate nanotubes with high adsorption capacities for lead and cadmium ions', *Chem. – A Eur. J.*, 2013, **19**, (5), pp. 1558–1562
[23] Qu J., Li W., Cao C.-Y., *ET AL.*: 'Metal silicate nanotubes with nanostructured walls as superb adsorbents for uranyl ions and lead ions in water', *J. Mater. Chem.*, 2012, **22**, (33), pp. 17222–17226
[24] Zhang M., Wu Y., Feng X., He X., Chen L., Zhang Y.: 'Fabrication of mesoporous silica-coated CNTs and application in size-selective protein separation', *J. Mater. Chem.*, 2010, **20**, (28), pp. 5835–5842
[25] Zhai Y., Zhai J., Zhou M., Dong S.: 'Ordered magnetic core-manganese oxide shell nanostructures and their application in water treatment', *J. Mater. Chem.*, 2009, **19**, (38), pp. 7030–7035
[26] Fei J.B., Cui Y., Yan X.H., *ET AL.*: 'Controlled preparation of MnO_2 hierarchical hollow nanostructures and their application in water treatment', *Adv. Mater.*, 2008, **20**, (3), pp. 452–456
[27] Dai Y., Lu X., McKiernan M., Lee E.P., Sun Y., Xia Y.: 'Hierarchical nanostructures of K-Birnessite nanoplates on anatase nanofibers and their application for decoloration of dye solution', *J. Mater. Chem.*, 2010, **20**, (16), pp. 3157–3162

doi: 10.1049/mnl.2013.0634